FAST LINEAR GEODESIC SHAPE REGRESSION USING COUPLED LOGDEMONS REGISTRATION

Zhuo Sun *Boudewijn P.F. Lelieveldt* *Marius Staring*

Division of Image Processing, Department of Radiology, Leiden University Medical Center, 2300 RC Leiden, The Netherlands

ABSTRACT

Longitudinal brain image series offers the possibility to study individual brain anatomical changes over time. Mathematical models are needed to study such developmental trajectories in detail. In this paper, we present a novel approach to study the individual brain anatomy over time via a linear geodesic shape regression method. In our method, we integrate separate pairwise registrations between the baseline image and the follow-up images into a unified spatial registration plus temporal regression framework. Different from previous geodesic shape regression approaches, which use the LDDMM framework to estimate the brain anatomical change over time, our method is based on the LogDemons method to decrease the computation cost, while maintaining the diffeomorphic property of the deformation over time. Moreover, a temporal regression constraint is explicitly implemented in each optimization iteration to make sure that the entire developmental trajectory can be compactly represented by the baseline image and an optimal stationary velocity field. Our method is mathematically well founded in the Alternating Direction Method of Multipliers (ADMM), which for our image regression application is interpreted in diffeomorphic space instead of Euclidean space. We evaluate our new method on 2D synthetic images and real 3D brain longitudinal image series, and the experiments show promising results in regression accuracy as well as estimated deformations.

Index Terms— stationary velocity field, shape regression, longitudinal brain image, LogDemons

1. INTRODUCTION

In the last 10 years, extensive research has been done on modeling the shape changes in longitudinal brain image series [1–3]. A standard solution is to directly extend pairwise registrations to longitudinal image series [1,4,5]. However, such piece-wise approaches often have jumps in the trajectory and fail to correctly represent anatomical development. To avoid these jumps, smooth kernel based methods [2] and geodesic shape regression methods [3] were proposed. While the former is more flexible, geodesic shape regression has a much clear physical meaning as a geodesic path passing through all images and can compactly represent the entire developmental trajectory by the baseline image and a single initial condition that determines the entire path.

In the computational anatomy field, the geodesic path between a pair of images can be computed depending on either the initial momenta (LDDMM [6]) or the stationary velocity field (SVF, e.g. LogDemons [7]). Currently, the geodesic shape regression methods [3, 8] only focus on the LDDMM framework, even though it is very time and memory consuming.

In this paper, we propose a new linear shape regression model based on the symmetric LogDemons method for longitudinal images. Our method has three advantages. Firstly, our method can be computed more efficiently than LDDMM based methods, owing to the LogDemons framework. Secondly, we propose a new iterative SVF merging step that enforces any pairwise deformation to follow a single trajectory. Thirdly, our method is mathematically well founded in the Alternating Direction Method of Multipliers (ADMM).

2. METHOD

2.1. Preliminaries

In our approach, the developmental trajectory is determined by a single initial SVF. As mentioned in [7], the LogDemons method extends the classical Demons model into the Log-Euclidean domain. The entire deformation path can be represented as the tangent space SVF v and the time interval t, using the exponential map $\phi(v,t) = Exp(v,t)$. This is equivalent to the unit time interval geodesic path with re-scaled velocity field $\phi(v,t) = Exp(v,t) = Exp(v \times t, 1)$, according to [9].

Since the exponential map guarantees to move a point from the tangent space of a manifold to the manifold itself, the trajectory of $\phi(v,t)$ is guaranteed to be always on the image manifold and the geodesic path determined by the SVF.

2.2. Linear Geodesic Shape Regression

The linear geodesic shape regression is an extension of least square regression from Euclidean space to diffeomorphic

978-1-4799-2374-8/15/$31.00

space, and it seeks to minimize the sum of squared differences between the measured and the predicted image, while keeping the deformation diffeomorphic. For a given longitudinal image list $\{I_0, I_1, I_2, .., I_N\}$ with scans at age $\{A_0, A_1, A_2, .., A_N\}$, the regression cost function can be written as:

$$E(\{\phi_1, \phi_2, .., \phi_N\}) = \sum_{i=1}^{N} \|I_i - I_0 \circ \phi_i\|_{L_2}^2 + Reg(\phi_i), \quad (1)$$

where ϕ_i is the deformation from baseline image I_0 to follow-up image I_i, and the regularization of the deformation field $Reg(\phi_i)$ is used to encourage the deformation to be diffeomorphic.

In our approach, we assume that brain shape changes according to a tangent space SVF, and we use the log-domain trajectory SVF v_0 to compactly define the entire geodesic deformation path

$$\phi(v_0, t) = Exp(v_0, t) = Exp(v_0 \times t, 1). \quad (2)$$

Instead of regularizing the deformation ϕ_i, we regularize the velocity field $v_0 \times t_i$, and we obtain a new regression cost function (1) in the log-domain:

$$E(v_0) = \sum_{i=1}^{N} \|I_i - I_0 \circ Exp(v_0 \times t_i, 1)\|_{L_2}^2 + Reg(v_0 \times t_i) \quad (3)$$

where the age interval $t_i = A_i - A_0$.

To compute the optimal trajectory SVF v_0 more efficiently, we first introduce new variables $v_i = v_0 \times t_i$ and replace $v_0 \times t_i$ by v_i to transfer the log-domain cost function (3) into a global variable consensus optimization problem [10], with product space variable $w = \{v_1, v_2, \ldots, v_N\}$ and the feasible region $\mathcal{C} = \{(v_1, v_2, \ldots, v_N) | v_i = v_0 \times t_i\}$.

To solve the shape regression problem in the diffeomorphic space, we interpret the scaled form ADMM method [10] in diffeomorphic instead of Euclidean space, by replacing the augmented Lagrangian term $\|v_i = v_0 \times t_i\|_2^2$ with function $Dist(v_1, v_2) = \|Log(Exp(-v_1) \circ Exp(v_2))\|_{L_2}^2$ for the geodesic distance. Then the diffeomorphic space augmented Lagrangian form is written as

$$\begin{aligned} L_\rho(\{v_i\}, v_0, \{u_i\}) = \sum_{i=1}^{N} [\|I_i - I_0 \circ Exp(v_i, 1)\|_{L_2}^2 \\ + Reg(v_i) + (\frac{\rho}{2}) Dist(v_i, v_0 \times t_i - u_i)] + g(v_0), \end{aligned} \quad (4)$$

where u_i is defined as scaled dual variable of the original dual variable y_i and $u_i = \frac{1}{\rho} y_i$. $dist(v_i, v_0 \times t_i - u_i)$ is the geodesic distance between the SVF v_i and $v_0 \times t_i - u_i$, and $g(v_0)$ encodes the feasible region constraint $\mathcal{C}$.

In order to solve this hard constraint problem (4), we use the ADMM method:

$$\begin{aligned} v_i^{k+1} = \underset{v_i}{\operatorname{argmin}} [\|I_i - I_0 \circ Exp(v_i, 1)\|_{L_2}^2 + Reg(v_i) \\ + (\rho/2)\, Dist(v_i, v_0^k \times t_i - u_i^k)] \end{aligned} \quad (5)$$

$$v_0^{k+1} = \prod_{\mathcal{C}} \{v_1^{k+1}, \ldots, v_N^{k+1}\} + \{u_1^{k+1}, \ldots, u_N^{k+1}\} \quad (6)$$

$$u_i^{k+1} = u_i^k + v_i^{k+1} - v_0^{k+1} \times t_i \quad (7)$$

$$v_i^{k+1} = u_i^{k+1} + v_0^{k+1} \times t_i, \qquad u_i^{k+1} = 0 \quad (8)$$

For Equation (5), it minimizes the sum of three terms: the image intensity difference, the deformation update distance and the vector field smoothness. Comparing to [7], we can see that these three terms are also used to define the LogDemons energy. By setting $\frac{\rho}{2} = \frac{\sigma_i}{\sigma_x}$, where σ_i is related to the noise of image and σ_x related to the uncertainty of spatial match, the minimization of v_i^{k+1} is equivalent to the optimization of the LogDomain Demons energy. The optimal v_i^{k+1} can therefore be efficiently computed using the symmetric LogDemons registration method [7].

For the second step (6), the projection $\prod_{\mathcal{C}}$ can be treated as finding the optimal element in the product space $\mathbf{W} = (\mathbf{V} \times \mathbf{V} \times ... \times \mathbf{V})$ in the feasible region $w^\star = \{v_0 \times t_1, v_0 \times t_2, ...v_0 \times t_N\}$ that minimizes the Euclidean distance to $w = \{v_1, v_2, ...v_N\}$. This projection operation on the product space $\mathbf{W}$ is equivalent to the least square regression problem in the original velocity field space $\mathbf{V}$ and the optimal v_0^{k+1} is therefore computed as

$$v_0^{k+1} = \frac{\sum_{i=1}^{N} t_i \times v_i^{k+1}}{\sum_{i=1}^{N} t_i^2}. \quad (9)$$

For the last step (7,8), the algorithm just projects the product space point $w = \{v_1, v_2, ...v_N\}$ onto the feasible region and then transfers it back to the original velocity field space $\mathbf{V}$:

$$v_i^{k+1} = v_0^{k+1} \times t_i. \quad (10)$$

After computing the trajectory SVF $v_0 = v_0^{k+1}$, the deformation from the baseline image to the follow-up image at any time point t can be computed as $\phi(v_0, t) = Exp(v_0, t)$ and we can interpolate or extrapolate the image I_t at time t as $I_t = I_0 \circ Exp(v_0, t)$.

2.3. Algorithm Summary

To deal with the large deformation and compute the linear shape regression more efficiently, we add a multi-resolution strategy into the method. The entire pipeline is summarized in Algorithm 1.

3. EXPERIMENT AND RESULT

3.1. Synthetic images experiment

To test if our shape regression method can model image changes, our first experiment is on the 2D synthetic binary bull's eye image series, shown in Fig. 1, where the motion is well captured using our method.

Data: longitudinal images $I_0, I_1, I_2, \ldots, I_N$ and scan age, resolution number, max iterations
Result: Trajectory SVF v_0
forall the *resolutions* **do**
  down-sample $I_i, \forall i$
  if *the lowest resolution* **then**
    $v_0^0 = Id$
  else
    up-sample v_0
  end
  forall the *iterations* **do**
    forall the *follow-up images* **do**
      compute v_i^{k+1} based on v_i^k, using LogDemons [7],
    end
    compute v_0^{k+1} based on v_i^{k+1}, using Equation (9)
    forall the *follow-up images* **do**
      $v_i^{k+1} \leftarrow v_0^{k+1} \times t_i$, using Equation (10)
    end
  end
  $v_0 \leftarrow v_0^{k+1}$ and $v_i \leftarrow v_i^{k+1}$
end

Algorithm 1: Multi-resolution linear geodesic shape regression

Our second experiment is on a square moving from left to right with vertical oscillations, shown in Fig. 2. In this experiment, we compare our iterative merging approach with a final merging approach [8], which computes v_0 (see (6)) only after the full registrations. From the result, we can see that iterative merging matches better and maintains the rigidity of the square. We repeat this experiment with more time samples, which indeed improves our regression results, see Fig. 3.

To quantify the non-rigidity in the mesh inside the square, we compute the standard deviation of the Jacobian determinant of the obtained deformations from the two previous motion of square experiments, and show the result in Table 1.

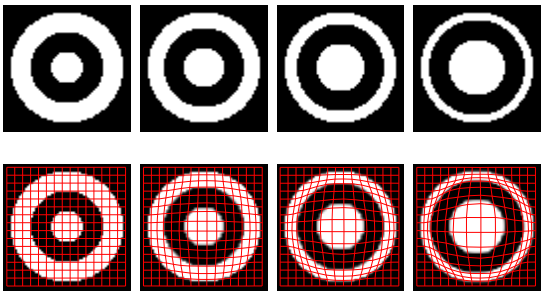

Fig. 1. Synthetic bulls eye experiment images (top row), results of geodesic shape regression (Bottom row), the result deformation field is shown with the red mesh.

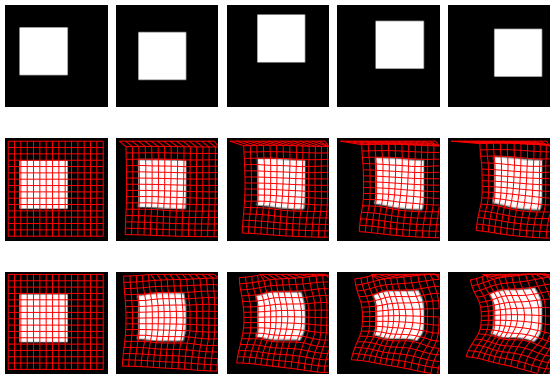

Fig. 2. Motion of a square. First row: follow-up images; Second row: predicted images using iterative merging; Third row: predicted images using final merging.

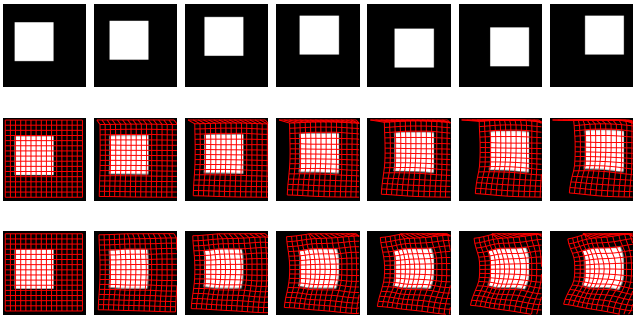

Fig. 3. Motion of a square with more sample points.

3.2. Real brain images

We also validate our linear shape regression method on a real 3D brain longitudinal image series from the ADNI dataset (`adni.loni.usc.edu`)(SubID 033_S_0514). All the longitudinal images are rigidly aligned to the baseline image first. Then we use all the brain images in the time-series to compute a linear regression model to fit all the images with the proposed iterative merging method. The result is given in Fig. 4, showing that the proposed method captures the ventricle expansion well.

Table 1. Std of the Jacobian determinant inside the square,with different sample numbers and merging methods

	im 1	im 2	im 3	im 4	im 5	im 6
5-iter	0.020	0.035	0.050	0.049		
5-final	0.074	0.143	0.222	0.249		
7-iter	0.013	0.021	0.026	0.030	0.061	0.077
7-final	0.039	0.077	0.113	0.144	0.187	0.215

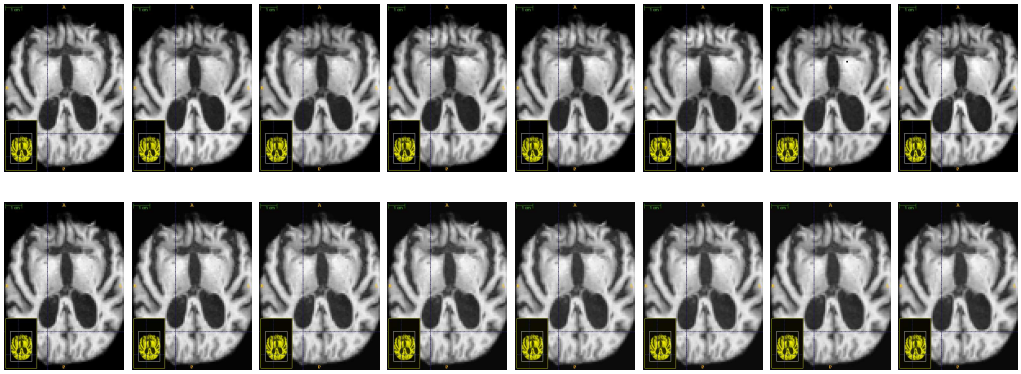

Fig. 4. Experiment of our linear shape regression method on real 3D brain data (age range: $80.9 - 85.9$). The blue focus lines indicate the same position in the image domain. Row 1: follow-up images; Row 2: prediction using the proposed method.

3.3. Compare pairwise velocity spread

To show the different behavior of the iterative and final merging strategies, we measure how well each pairwise deformation follows a single deformation path. To this end we compute the so-called generalized variance, i.e. the determinant of the co-variance of the unit time pairwise SVF's before merging: $Spread(\{v_i\}) = \text{mean}(\det(\text{cov}(\{v_i(x)/t_i\})))$. The result is given in Fig. 5, showing that the proposed method better aligns the pairwise SVFs to the common direction, where the spread was reduced with several orders of magnitude.

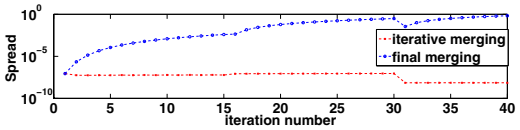

Fig. 5. Log-plot of inter-pair unit time velocity field spread

4. CONCLUSION

In this paper, we present a new fast linear geodesic shape regression method. By introducing the ADMM framework, we rebuild the shape regression problem as a list of independent LogDemons problems, which are coupled in every iteration. Experiments on both 2D synthetic images and a 3D brain longitudinal image series show that the proposed method is promising in modeling longitudinal shape changes. Based on the LogDemons method, our linear geodesic shape regression method is much faster than the traditional LDDMM-based geodesic shape regression methods.

5. REFERENCES

[1] A. Serag et al., "Lisa: Longitudinal image registration via spatio-temporal atlases," in *ISBI*, 2012, pp. 334–337.

[2] B. Davis et al., "Population shape regression from random design data," *International journal of computer vision*, vol. 90, no. 2, pp. 255–266, 2010.

[3] M. Niethammer et al., "Geodesic regression for image time-series," in *MICCAI*, pp. 655–662. 2011.

[4] S. Durrleman et al., "Spatiotemporal atlas estimation for developmental delay detection in longitudinal datasets," in *MICCAI*, pp. 297–304. 2009.

[5] M. Niethammer et al., "An optimal control approach for the registration of image time-series," in *CDC/CCC*, 2009, pp. 2427–2434.

[6] M. Beg et al., "Computing large deformation metric mappings via geodesic flows of diffeomorphisms," *International journal of computer vision*, vol. 61, no. 2, pp. 139–157, 2005.

[7] T. Vercauteren et al., "Symmetric log-domain diffeomorphic registration: A demons-based approach," in *MICCAI*, pp. 754–761. 2008.

[8] Y. Hong et al., "Simple geodesic regression for image time-series," in *Biomedical Image Registration*, pp. 11–20. 2012.

[9] M. Lorenzi et al., "Geodesics, parallel transport & one-parameter subgroups for diffeomorphic image registration," *International journal of computer vision*, vol. 105, no. 2, pp. 111–127, 2013.

[10] S. Boyd et al., "Distributed optimization and statistical learning via the alternating direction method of multipliers," *Foundations and Trends in Machine Learning*, vol. 3, no. 1, pp. 1–122, 2011.